  Bull. Chem. Soc. Jpn., 56, 3715—3721 (1983)

Studies on the Mechanism of Zeolite X Crystallization. I. Effects of Silica Sources of Starting Materials on the Crystallization of Zeolite X

Ryozi Hino,* Ryohei Matuura,† and Kenzi Toki

Department of Chemistry, Faculty of Science, Shimane University, Nishikawatsu, Matsue 690

†*Department of Chemistry, Faculty of Science, Kyushu University, Hakozaki, Higashi-ku, Fukuoka 812*

(Received January 6, 1983)

The crystallization mechanism for zeolite was investigated. Tetraethyl orthosilicate and silica sol were used as silica sources. Many kinds of solid phases were obtained at various reaction times. These solid phases were characterized by analyses for chemical compositions, X-ray diffraction, adsorption of nitrogen gas and water vapor, and IR spectroscopy. The results obtained suggest that the solid phase derived from tetraethyl orthosilicate at an early stage of reaction is composed of slightly ordered skeletons. In addition, during aging of gel at room temperature, the structure of the solid phase of gel undergoes a rearrangement to form a crystalline structure. On the other hand, the gel phase obtained from silica sol is predominantly made up by the coagulation of disordered aluminosilicate polymers or silicic polymers. These gel phases act as a precursor, and a part of the gel dissolved into the liquid phase and the dissolved species are converted into crystals in the liquid phase. Thus, the silica sources influence the structure of gel and crystals. In general, the crystallization mechanism is strongly influenced by the starting materials, especially by the silica sources.

Many investigation on the mechanism and kinetics of zeolite crystallization have been done in recent years. These investigations are concerned with autocatalysis[1] and effects of temperature,[2] alkalinity,[2,3] and seeding,[1] and kinetically have dealt with the conversion from amorphous substances to crystals[4-9] and induction periods with respect to the distribution of chemical species in liquid and solid phases.[10-12] In addition, Raman[5] and IR[13,14] spectra of liquid and solid phases of gel were analyzed in order to understand the zeolite crystallization.

However, because of complex reactions of aluminosilicate in liquid and solid phases, the process of zeolite crystallization has not yet been made clear.

Schwochow and Heinze[15] reported that zeolite A, sodalite, zeolite P, and faujasite were crystallized from a liquid phase which had been separated from an aluminosilicate gel phase during a crystallization process. Zhdanov[11] revealed that the liquid phase of aluminosilicate gel influenced properties and compositions of crystals formed.

On the other hand, many investigations have revealed that the crystallization of zeolite occurs in the solid phase of gel through rearrangement of alumonisilicate framework. For example, Khatami and Flanigen[16] observed that the crystallization of gel phase occurred in the absence of liquid phase. After all, at the present stage there have been proposed two mechanisms for the zeolite crystallization based on two representative hypotheses. The first mechanism is based on a crystallization to occur in a solid phase. During the aging of this solid phase a rearragement of the aluminosilicate framework leads the amorphous gel to crystals. This mechanism is supported by Breck and Flanigen,[7] McNicol *et al.*,[17] and Aiello *et al.*[18]

The other mechanism is based on a crystallization to occur in a liquid phase; the constituents of zeolite are caused to be dissolved into a liquid phase *via* their precursors, amorphous gel phases, and then zeolite is made crystallized in a liquid phase. This mechanism is supported by Kerr,[1] Ciric,[9] Culfaz and Sand,[4] and Kacirek and Lechert.[19]

In our previous papers we reported that syntheses of zeolite A[20] and zeolite X[21] using tetraethyl orthosilicate as a silica source could proceed easily. These zeolites, in crystal, had a high purity and a high crystallinity. In addition, we investigated the difference between the distributions of component concentrations in the solid and liquid phases during processes of zeolite crystallization using tetraethyl orthosilicate, silica sol,[21] or sodium metasilicate.[22] These results suggested that at the beginning of reaction, the difference in the silica sources has an influence on chemical states of the soluble species of constituents of zeolite in the liquid phase, together with a significant influence on the nucleation of zeolite crystals, growth steps of aluminosilicate, and properties of crystals produced.

In the present study, solid phases were sampled out of reaction systems at various reaction times. These solid phases were characterized by chemical analysis, X-ray diffraction, adsorption of nitrogen gas and water vapor, and IR spectra. These results were compared with earlier results.[21]

Experimental

Materials. The silica sources used were a commercial tetraethyl orthosilicate (Nakarai Chemical Co. Ltd.) purified by distillation, and a silica sol which had been prepared by diluting a Snowtex 40 (Nissan Chemical Co. Ltd.) with distilled water to double the volume. The alumina source used was a sodium aluminate solution which had been synthesized from Al plate (99.99%, Nakarai Chemical Co. Ltd.) and sodium hydroxide solution. A sodium hydroxide solution (5 mol dm^{-3}) was used as excess alkaline solution. These starting materials were described in detail elsewhere.[21]

Preparation of Specimens. The molar ratios of SiO_2/Al_2O_3, Na_2O/SiO_2, and H_2O/Na_2O adopted for the preparation of mixtures of starting materials were 8, 6, and 50, respectively, which correspond to the formula $48Na_2O \cdot Al_2O_3 \cdot 8SiO_2 \cdot 2400H_2O$. These ratios have been established as falling in the region providing optimum conditions for the synthesis of zeolite X.[23]

The procedure of synthesis was as follows. Tetraethyl orthosilicate was added to a sodium aluminate solution in a flask, and the mixture was stirred by an ultra sonic generator (40 kHz) for 20 min. A mixture of sodium hydroxide solution and distilled water was added to the flask and allowed to be stirred mechanically for 6—72 h at room temperature. To prevent evaporation the flask was equipped with a glass tubing with both ends open, and it was heated in an air oven at 85 °C for 74—96 h. After a fixed time, the solid and liquid phases of reaction mixture were separated with a centrifuge. The supernatant solution of the liquid phase was pipetted out as a specimen of the liquid phase. The solid phase was filtered and washed with distilled water until the pH of washings reached 10.5 and then dried at 110 °C for 24 h.

Analyses. Analyses of liquid and solid phases were made as follows. The colorimetric method, *i.e.*, the molybosilicic acid yellow method, and a Hitachi spectrophotometer model 100-30 were applied to determining silica concentrations. Flame photometry using a Hitachi atomic absorption analyzed model 208 was applied to determining sodium concentrations. Aluminium concentrations were determined by the chelatometric titration using EDTA and Zn standard solutions and an XO indicator.

Adsorption. The adsorption of nitrogen gas was subjected to volumetric measurements at the boiling point of liquid nitrogen and the adsorption of water vapor to gravimetric measurements at 25 °C. The pretreatment of specimens was carried out as follows. After being kept at 110 °C for 24 h, the specimen was heated at 300 °C for 2 h under atmospheric pressure, and degassed under vacuum (at 10^{-5} mmHg) (1 mmHg≈133.322 Pa) for 30 min prior to the adsorption.

IR Spectra. Infrared transmission spectra were measured by the KBr wafer technique according to the study by Flanigen and Khatami.[13] Every wafer contained 1 mg of solid phase in 300 mg of KBr. Spectra were recorded on a Hitachi infrared spectrometer model 260-50.

Crystallinity. Products were identified by the powder X-ray diffractometry using a Toshiba X-ray diffractometer model ADG 301 (Cu *Kα*, Ni filter, 30 kV, 20 mA, G. M. detector) and a JEOL model JDX-7E (Cu *Kα*, Ni filter, 30 kV, 20 mA, scintillation counter). The crystallinity was determined by the X-ray diffraction method with an LMS 13X as reference.

Results

Crystallinity. The solid phase derived from tetraethyl orthosilicate remained amorphous for initial 75 h after the beginning of reaction, but began to include crystals at 76 h. The solid phase derived from silica sol remained amorphous for initial 74 h, but began to inculude crystals at 75 h. Table 1 shows the change in crystallinity with reaction time. The change in crystallinity proceeded very rapidly immediately after crystals were recognized in the solid phase from either tetraethyl orthosilicate or silica sol, and the rate of crystallization decreased after a few hours. Then, the crystallinity was kept almost constant.

The crystals derived from tetraethyl orthosilicate and from silica sol showed relative crystallinities of 120 and 75%, respectively, and the interplanar spacings of planes (111) as measured by X-ray diffraction were 14.27—14.25 and 14.23—14.14 Å, respectively. The crystal derived from silica sol increased in interplanar spacing

Table 1. Change/% in crystallinity[a)]

Reaction time/h	74	75	76	78	84	96
Silica source						
Tetraethyl orthosilicate	0	0	43	115	122	115
Silica sol	0	48	75	70	76	77

a) Reference standard, LMS 13X: 100%.

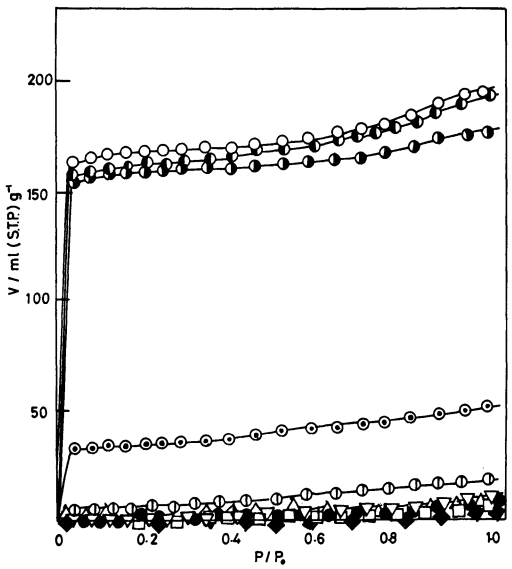

Fig. 1. Adsorption isotherms of nitrogen gas on the solid phases (E) derived from tetraethyl orthosilicate at −196 °C. 96E: ◐, 84E: ○, 78E: ◑, 76E: ⊙, 75E: ⊕, 74E: □, 72E: ●, 48E: △, 24E: ◆, 6E: ▽.
Number: reaction time.

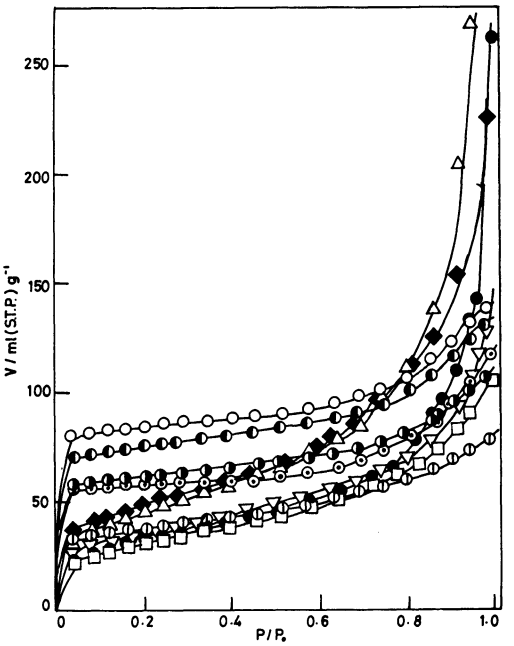

Fig. 2. Adsorption isotherms of nitrogen gas on the solid phases (C) derived from silica sol at −196 °C. 96C: ◐, 84C: ○, 78C: ◑, 76C: ⊙, 75C: ⊕, 74C: □, 72C: ●, 48C: △, 24C: ◆, 6C: ▽.
Number: reaction time.

with increasing crystallinity.

Adsorption of Nitrogen Gas. Figures 1 and 2 show nitrogen gas adsorption isotherms for solid phases. The solid phases are grouped in three types according to the stage of their formation: the initial amorphous stage (6E—75E, 6C—74C), the early stage of crystallization (76E, 75C), and the full-crystallization stage (78E—96E, 76C—96C). The solid phase derived from tetraethyl orthosilicate shows the isotherms that run nearly parallel with the axis of relative pressure. Although the amorphous phases adsorb little nitrogen, the amount adsorbed increased rapidly immediately after the crystals began to be observed.

On the other hand, the solid phases derived from silica sol show adsorption isotherms a little different from those for tetraethyl orthosilicate. The amorphous state (6C—74C) shows somewhat a steep slope as compared with the former at lower relative pressures. The amount adsorbed is 25—40 ml/g in contrast to the solid phases (6E—75E) which adsorb little. This does not result from a difference, if any, in the developments of internal structure, but actually has arisen from different distributions of particle size. The particle sizes measured with a particle size analyzer and a scanning electron micrograph were 1.5—25 μm (av 6.6 μm) for 72E and 0.25—10 μm (av 2.4 μm) for 74C. The solid phases derived from silica sol indicate distributions of smaller particles.

At lower relative pressures, the slopes to the adsorption isotherms for the crystalline phases (75C—96C) are similar to those for tetraethyl orthosilicate (76E—96E). Although the amount adsorbed by the latter is *ca.* 160—170 ml/g, the former adsorb *ca.* one third of this value, *i.e.*, 50—70 ml/g. Such characteristics of adsorption isotherms are influenced by the presence of a large amount of an amorphous substance, aluminosilicate gel, which is always contaminated.

The monolayer capacity and specific surface area were calculated with the Langmuir or BET equation. The results of calculation are shown in Table 2. The outer and inner surface areas are tabulated in the same table. These values were evaluated by fitting the Frenkel-Halsey-Hill equation[24,25] to experimental data.

The change in inner and outer specific surface areas is shown in Fig. 3. The solid phases derived from tetraethyl orthosilicate remained amorphous for initial 75 h of reaction time, so that these solid phases adsorb so little as to give an inner specific surface area of zero. Their outer specific surface areas are 4—5 m^2/g. The solid phase which contained crystals rapidly increased in specific surface area with reaction time, up to over 700 m^2/g. Nearly 95% of this value is dependent on the inner structure of crystals. The remaining *ca.* 5% is attributable to the outer free surface of solid phase. On the other hand, in spite of the amorphous state, the amount adsorbed by the solid phases derived from silica sol is nearly 100—150 m^2/g, with no inner specific surface area detected. The specific surface area did not remarkably increase with reaction time after crystalline substances had appeared. Their values are *ca.* 250—300 m^2/g.

The outer specific surface area decreases slightly after the solid phase begins to crystallize. But it occupies *ca.* 15—25% of the total specific surface area. Its value is 40—70 m^2/g, and the outer surface areas for the solid phases derived from silica sol are larger than those for tetraethyl orthosilicate. It may be considered that in the course of crystallization the size of crystals can grow to some extent. Because of the crystals being contaminated with a large amount of amorphous substances as mentioned above, their outer surface areas amount to a larger portion of the total surface area.

Adsorption of Water Vapor. The diameter of water molecule (2.7 Å at 25 °C) is smaller than that of nitrogen molecule (3.64 Å at −196 °C). Water molecule is polar and is expected to be adsorbed fully on fine

Table 2. Results of adsorption of nitrogen gas

Specimen	V_m [a] / ml g^{-1}	S_s [b] / m^2 g^{-1}	S_i [c] / m^2 g^{-1}	S_e [d] / m^2 g^{-1}	S_i+S_e [e] / m^2 g^{-1}
96E	165	717	633	59	692
84E	171	746	690	35	725
78E	162	708	657	30	687
76E	105	457	385	45	430
75E	4	19	6	13	19
74E	1	4	0	5	5
72E	2	7	0	5	5
48E	1	3	0	3	3
24E	1	4	0	4	4
6E	1	4	0	4	4
96C	74	324	226	78	304
84C	84	366	303	50	353
78C	59	257	185	62	247
76C	58	251	219	26	245
75C	32	141	74	74	148
74C	25	107	0	103	103
72C	26	112	0	109	109
48C	36	159	0	150	150
24C	40	174	0	165	165
6C	28	123	0	120	120

a) V_m is the monolayer capacity. b) S_s is the specific surface area. c) S_i is the inner specific surface area. d) S_e is the outer specific surface area. e) S_i+S_e is the sum of inner and outer specific surface areas.

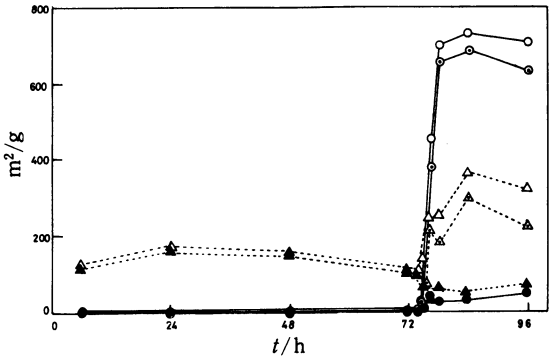

Fig. 3. Changes of the specific surface area obtained from the adsorption of nitrogen gas. Solid and dotted line represent the solid phase derived from tetraethyl orthosilicate and from silica sol respectively.
—◐— ---△---: Total specific surface area,
—⊙— ---◬---: inner specific surface area,
—●— ---▲---: outer specific surface area.

structures of zeolite. Therefore, the method using water molecule is more effective for the study on the change in the solid phase than the method using nitrogen gas only. Some of the adsorption isotherms obtained are shown in Fig. 4. The crystals (96E, 84E) adsorb water vapor in fairly large quantities, and the slopes to adsorption isotherms are smooth, as compared with those for the crystals derived from silica sol. The amorphous substance (72E) adsorbs little water vapor.

On the contrary, the amorphous substance (72C) adsorbs water vapor in a fairly large quantity at lower relative pressures. Such a trend of adsorption isotherms is similar to that observed in the case of nitrogen adsorption by amorphous solid phases. The specific surface areas evaluated from the water vapor adsorption have revealed that the solid phases (96E, 84E) have larger values than the solid phases (96C, 84C). The high crystalline phases (96E, 84E, 96C) have larger specific surface areas by *ca.* 200—250 m^2/g than the corresponding values determined by nitrogen adsorption. Similarly the solid phases (84C, 72C) also have indicated larger values by *ca.* 100—150 m^2/g.

IR Spectra. A systematic study of infrared spectra for the characterization of zeolite frameworks with respect to crystal structure has been done by Flanigen and Khatami.[13,26] They pointed out that the mid-infrared region (1300 to 250 cm^{-1}) contains the fundamental vibrations of the framework of zeolite. The mid-infrared vibrations of zeolite were classified into two groups by them. One is the internal vibrations that are insensitive to change in the framework structure, and the other is the external vibrations that are sensitive to change in the framework.

The change in infrared spectra in going from the amorphous solid phase to crystals are shown in Figs. 5 and 6. The features of the spectra obtained for the specimens derived from tetraethyl orthosilicate are as follows:

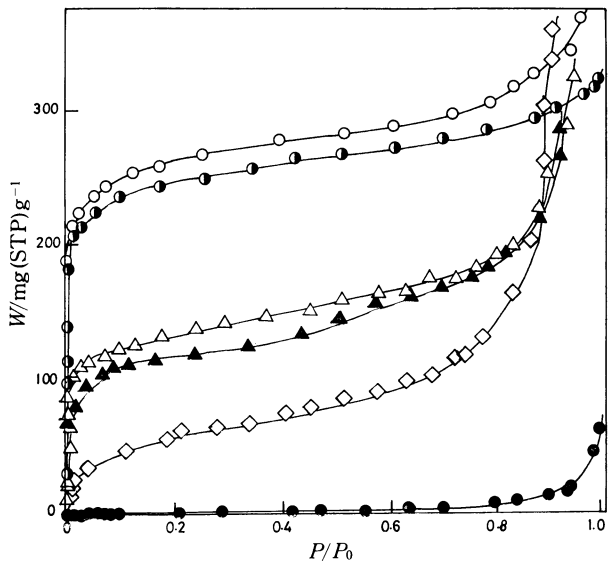

Fig. 4. Adsorption isotherms of water vapor at 25 °C. 96E: ○, 84E: ◑, 72E: ●, 96C: △, 84C: ▲, 72C: ◇. E: Tetraethyl orthosilicate, C: silica sol. Number: reaction time.

1) The spectra for earlier stages (6E, 24E) bear a resemblance to those of the crystals of high crystallinity.

2) The strongest vibration around 1000 cm^{-1} that is common to all zeolites and assigned to an asymmetric stretching mode ←OT→←O (T represents Si or Al) is found near 1000 cm^{-1} (6E—75E), but the frequency shifts to 980 cm^{-1} (76E—96E). The change in frequency shift is much less than that for the spectra of the solid phases derived from silica sol.

3) The amorphous specimens show very weak and broad bands around 580 cm^{-1}. The feature of this band in this region has a clearer pattern than the corresponding spectra for silica sol. The band in 650—500 cm^{-1} is assignable to a double 6-ring. But this band is obscure as compared with other bands in the spectrum. The crystals (76E—96E) show the clear band due to the double 6-ring around 560 cm^{-1}. The change in these bands suggests that the amorphous solid phases in the gel are composed of frameworks of secondary building units loosely cross-linked with aluminosilicate anions; therefore, the solid phases are converted from the amorphous solid state to a crystalline substance through the rearrangement of the bonds of aluminosilicate

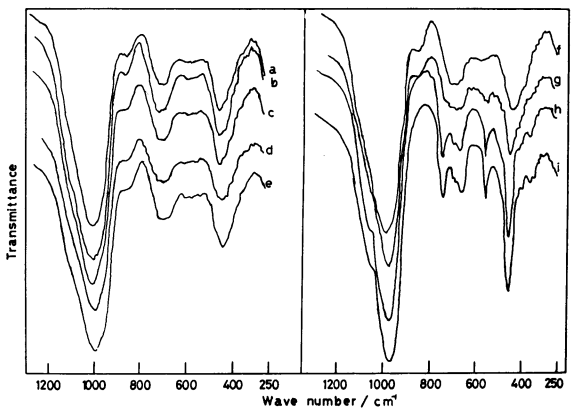

Fig. 5. Mid-infrared spectra of the solid phases (E) derived from tetraethyl orthosilicate. a: 6E, b: 24E, c: 48E, d: 72E, e: 74E, f: 75E, g: 76E, h: 78E, i: 84E, 96E.
Number: reaction time.

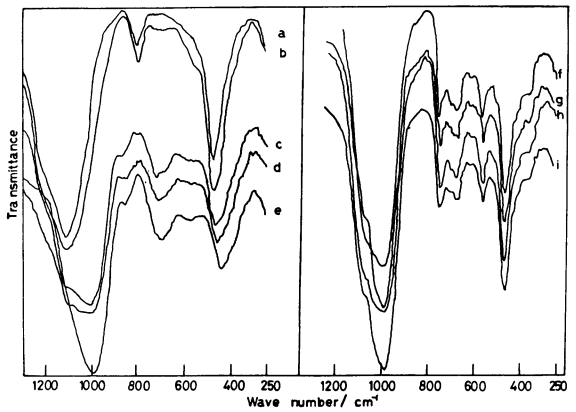

Fig. 6. Mid-infrared spectra of the solid phases (C) derived from silica sol. a: 6C, b: 24C, c: 48C, d: 72C, e: 74C, f: 75C, g: 76C, h: 78C, i: 84C, 96C.
Number: reaction time.

polymers by the interaction between the solid and liquid phases of gel.

4) The band at 880 cm^{-1} assigned to Si–OH is found with the specimens (6E—76E). This band is no longer found with the specimens (78E—96E). This suggests that the amorphous solid state is caused to change into crystals that have high crystallinity through the combination of secondary building units with aluminosilicate polymers.

5) The spectral shape of the strongest asymmetric stretching around 1000 cm^{-1} is almost the same for all the specimens, in contrast with those derived from silica sol.

On the other hand, the features of the spectra for the specimens derived from silica sol are as follows:

1) The spectra are classified into three groups. The first group is for the amorphous substances obtained at earlier stages of reaction (6C, 24C). The second is for the specimens which have undergone aging for a pretty long term (48C, 72C, 74C). The third is for the crystalline substances. The infrared spectra of the first group have very simple patterns.

2) The first group has the strongest band around 1120 cm^{-1}, shifting to lower frequencies, 1040 and 1020 cm^{-1} for 48C and 72C, respectively. As a whole, the specimens (6C—72C) show broad spectra composed of many bands. This suggests that the solid phase consists of a large quantity of silica; in addition, it contains many varieties of siloxane and Al–O–Si bonds contaminated with the zeolite framework. This band is observed around 1000 cm^{-1} for 74C and around 990 cm^{-1} for 75C and 76C. The band is remarkably shifted to lower frequencies, as compared with the band observed in the case of tetraethyl orthosilicate.

3) The bands for the double 6-ring and pore opening have been observed in the specimen (75C) for the first time.

4) The band for the Si–OH vibration around 880 cm^{-1} is still observed in the crystalline specimen (78C). It becomes weak as the crystallization proceeds. But the very weak band remains in the spectra of crystals. On the contrary, no trace of that band is observed in the spectra of the crystals derived from tetraethyl orthosilicate. This suggests clearly that the former crystals will not grow sufficiently, and that they includes some nonbonding structures and amorphous substances

Discussion

In our previous study[21] on the mechanism of zeolite crystallization, we investigated the difference in constituents between the liquid and solid phases which had been derived from tetraethyl orthosilicate, sodium metasilicate, and silica sol as silica sources with various reaction times. In order to clarify the chemical bonding state of constituents in the solid phases, the dissolution of constituents of the solid phase into hydrochloric acid solution and the relative concentration of constituents dissolved were surveyed.

According to the findings obtained, the change in constituents of both the liquid and solid phases derived from silica sol is abrupt as compared with the solid phases derived from tetraethyl orthosilicate and sodium metasilicate. The X-ray amorphous phases derived from silica sol consists of silica predominantly, and alumina or soda is hardly incorporated in the framework. The change in constituents of both the liquid and solid phases derived from tetraethyl orthosilicate is slow, and as a whole the behavior of all constituents is similar to one another. X-Ray amorphous phases obtained at earlier stages of reaction bear a marked resemblance to crystals with respect to constituents. A similarity among the solid phases obtained at various reaction times is found in respect of the dissolution of constituents of the solid phase into hydrochloric acid solution. On the contrary, every solid phase derived from silica sol shows a markedly different behavior of dissolution.[21] These results suggest that the framework structure and chemical-bond features of the solid phases are markedly dependent on the silica sources used. The X-ray amorphous phase derived from tetraethyl orthosilicate is composed of somewhat similar ordered skeletons of aluminosilicate which constitute the chemical structure of crystalline phase. On the other hand, the coexistent phase derived from silica sol is composed of disordered skeletons of aluminosilicate.

It is considered that these results are due to the difference in both the gelation kinetics and the structure of aluminosilicate at the beginning of reaction. Thus, in the case of tetraethyl orthosilicate, the gelation kinetics is governed by the polymerization of ordered aluminosilicate which has grown up in the solution. On the contrary, in the case of the solid phase derived from silica sol, the dominant factor governing the gelation kinetics is the aggregation of disordered aluminosilicate polymers.

In spite of the solid phase consisting of disordered aluminosilicate skeletons derived from silica sol, the beginning of crystallization occurs about one hour earlier than in the case of tetraethyl orthosilicate. As shown in Table 1, the crystallization does not proceed so far as expected, and the crystallinity is *ca.* 60—70% in contrast with that derived from tetraethyl orthosilicate. This suggests that in the case of silica sol, the gelation kinetics is governed by the aggregation of aluminosilicate polymers and silicic polymers at the beginning of reaction, so that the nucleation of crystals takes place more rapidly so as to make the number of nuclei more than in the case of tetraethyl orthosilicate which is hydrolyzed slowly. These trends are consistent with the fact that the X-ray amorphous phase derived from silica sol is very viscous at the beginning of reaction. On the contrary, the X-ray amorphous phases derived from tetraethyl orthosilicate consists of particles of larger sizes.

Because the silica sol was originally prepared by dispersion of silicic polymer in water, it may be considered that the reaction of depolymerization-polymerization of silicic polymer during zeolite crystallization proceeds insufficiently. Therefore, the crystals obtained with silica sol are caused to include the aluminosilicate which will not participate in the crystal framework. In addition, it may be considered that the crystals formed have a fairly silica-rich structure. This is suggested from the fact that the diffractive angle 2θ of

X-ray diffraction peak (642) have values in the region 26.74—26.75° (lattice constant, a_0: 24.94—24.93 Å) for the specimens obtained from tetraethyl orthosilicate and in the region 26.81—26.84° (a_0: 24.88—24.85 Å) for the specimens obtained from silica sol. These results are consistent with the relation found between the Si/Al molar ratio and the lattice constant.[7] In addition, these results correspond also to the results[21] concerning the difference in constituent distribution between the liquid and solid phases.

According to the above discussion, the X-ray amorphous phase derived from tetraethyl orthosilicate is considered to have a structure of ordered skeletons, and therefore the development of cavities and channels in the solid phase may be expected at earlier stages of reaction. But it has been proved that any sufficient development of cavities and channels, which is detectable through the adsorption for nitrogen gas or water vapor, will not proceed in the amorphous solid state. This means that any crystallographic internal structures characteristic of zeolite cannot fully be constructed until crystals become recognized by X-ray diffraction.

Both the crystallinity and the amount adsorbed increase with reaction time, and the approximate specific surface areas evaluated for the crystals are 450 m^2/g for 76E, 710 m^2/g for 96E, 140 m^2/g for 75C, 250 m^2/g for 76C, and 360 m^2/g for 84C. These results suggest that the inner structure of the crystals derived from tetraethyl orthosilicate will grow about 2 to 3 times as much as that of the crystals derived from silica sol. The former crystals indicate a large difference between their specific surface areas measured with nitrogen gas and water vapor. These results show that the inner structure, especially the structure of micro pore, grows to a considerable extent in the crystals derived from tetraethyl orthosilicate as compared with those derived from silica sol. The different development of inner structure is in accord with the results concluding different degrees of crystallinity and different constituent distribution in both liquid and solid phases.

The infrared bands, called "external linkages"[13] and sensitive to the change in framework structure, become apparently detectable immediately after crystals have become observed. The spectrum obtained for the solid phase derived from each of the silica sources shows a very characteristic pattern. It is derivable from the change in spectra with reaction time that each solid phase is formed *via* its unique reaction mechanism.

The results obtained in the present study are in good agreement with the conclusion drawn in earlier tudies[21,22] that the X-ray amorphous phases obtained from tetraethyl orthosilicate at earlier stages are essentially identical with crystals.

The nucleation and nuclear growth are the most important steps for obtaining highly crystalline zeolites. The X-ray amorphous phases formed from tetraethyl orthosilicate are even initially composed of highly ordered structures; the subsequent interaction between the liquid and solid phases serves to raise the crystallinity during the aging time at room temperature. It thus follows that the crystals have high crystallinity and high purity. On the other hand, the X-ray amorphous phase derived from silica sol contains amorphous substances which cannot easily be removed from the solid phase during the aging time. Such behavior results from the structural characteristic of the gel itself. It may be considered that the X-ray amorphous phase derived from silica sol is made up predominantly *via* coagulation of aluminosilicate polymers or silicic polymers; that is, the amorphous substance as a precursor is allowed to deposit in the liquid phase. In addition, the constituent of zeolite is caused to get out of the gel during the aging time and the bond of Al–O–Si is formed newly. This is why the crystal phase coexists with a large amount of amorphous substance.

Breck[27] pointed out that the composition and structure of gel are controlled by the size and structure of polymerizing species. Since silicate may vary in chemical composition and molecular weight distribution, different silicate solutions may result in different gel structures. Therefore the gelation may control the nucleation of zeolite crystals. This sequence has strongly been supported in this study. In the zeolite synthesis, the kind of starting materials, particularly silica source, and the chemical state of gel phase strongly influence the crystallization mechanism.

The authors wish to express their thanks to Messrs. Hiroyasu Aoi and Kōzi Kitagawa for their assistance during the experiment.

References

1) G. T. Kerr, *J. Phys. Chem.*, **70**, 1047 (1966).
2) R. M. Barrer and E. A. D. White, *J. Chem. Soc.*, **1952**, 1561.
3) R. M. Barrer, J. W. Baynham, F. W. Bultitude, and W. M. Meier, *J. Chem. Soc.*, **1959**, 195.
4) A. Culfaz and L. B. Sand, *Adv. Chem. Sre.*, **121**, 140 (1973).
5) B. D. NcNicol, G. T. Pott, K. R. Loss, and N. Mulder, *Adv. Chem. Ser.*, **121**, 152 (1973).
6) W. Meise and F. E. Schwochow, *Adv. Chem. Ser.*, **121**, 169 (1973).
7) D. W. Breck and E. M. Flanigen, "Molecular Sieves," The Society of Chemical Industry, London (1968), p. 47.
8) S. P. Zhdanov and N. N. Samulevich, "Proceeding of the Fifth International Conference on Zeolites," Heyden and Son Ltd., London (1980), p. 75.
9) J. Ciric, *J. Colloid Interface Sci.*, **28**, 315 (1968).
10) S. P. Zhdanov, "Molecular Sieves," The Society of Chemical Industry, London (1968), p. 62.
11) S. P. Zhdanov, *Adv. Chem. Ser.*, **101**, 20 (1971).
12) F. Polak and A. Cichocki, *Adv. Chem. Ser.*, **121**, 209 (1973).
13) E. M. Flanigen and H. Khatami, *Adv. Chem. Ser.*, **101**, 201 (1971).
14) W. C. Beard, *Adv. Chem. Ser.*, **121**, 162 (1973).
15) F. E. Schwochow and G. W. Heinze, *Adv. Chem. Ser.*, **101**, 102 (1971).
16) H. Khatami and E. M. Flanigen, Union Carbide Corporation, unpublished results.
17) B. D. McNicol, G. T. Pott, and K. R. Loss, *J. Phys. Chem.*, **76**, 3388 (1972).
18) R. Aiello, R. M. Barrer, and I. S. Kerr, *Adv. Chem. Ser.*, **101**, 44 (1971).
19) H. Kacirek and H. Lechert, *J. Phys. Chem.*, **80**, 1291

(1976).
20) R. Hino and K. Toki, *Nippon Kagaku Kaishi*, **1975**, 1847.
21) R. Hino and K. Toki, *Nippon Kagaku Kaishi*, **1977**, 593.
22) R. Hino and K. Toki, *Mem. Fac. Lit. and Sci., Shimane Univ., Nat. Sci.*, **9**, 71 (1975).
23) R. Hino and K. Toki, *Mem. Fac. Lit. and Sci., Shimane Univ., Nat. Sci.*, **8**, 61 (1975).
24) M. Nakagaki, Y. Nakamura, and T. Fujie, *Yakugaku Zasshi*, **91**, 667 (1971).
25) P. L. Walker and W. V. Kotlensky, *Can. J. Chem.*, **40**, 184 (1962).
26) E. M. Flanigen, "Zeolite Chemistry and Catalysis," ACS Monograph 171, American Chemical Society, Washington, D. C. (1976), p. 80.
27) D. W. Breck, "Zeolite Molecular Sieves," John Wiley and Sons, New York (1973), Chap. 4, p. 339.